Characterization of Rayleigh backscattering arising in various two-mode fibers

Characterization of Rayleigh backscattering arising in various two-mode fibers

Dawei Yu,[1,2] Songnian Fu,[1,*] Zizheng Cao,[2] Ming Tang,[1] Lei Deng,[1] Deming Liu,[1] Ian Giles,[3] Ton Koonen,[2] and Chigo Okonkwo[2]

[1]*Wuhan National Laboratory for Optoelectronics, and School of Optical and Electronic Information, Huazhong University of Science and Technology, Wuhan 430074, China*
[2]*COBRA Research Institute, Eindhoven University of Technology, Eindhoven, 5612 AZ, Netherlands*
[3]*Phoenix Photonics, Sarre Business Centre, Canterbury Road, Sarre, Birchington, Kent CT7 0JZ, UK*
[*]*songnian@mail.hust.edu.cn*

Abstract: We experimentally characterize the mode dependent characteristics of Rayleigh backscattering (RB) arising in various two-mode fibers (TMFs). With the help of an all-fiber photonic lantern, we are able to measure the RB power at individual modes. Consequently, mode dependent power distribution of RB light caused by arbitrary forward propagation mode superposition can be obtained. The total RB power of the TMFs under test is higher than that of single mode fiber by at least 2 dB over the C band. Meanwhile, the RB light occurs among all guided modes in the TMFs with specific power ratios. The experimental characterization agrees well with the theoretical calculations.

OCIS codes: (060.2270) Fiber characterization; (290.5870) Scattering, Rayleigh; (060.2300) Fiber measurements; (290.5820) Scattering measurements; (290.1350) Backscattering.

References and links

1. E. Brinkmeyer, "Analysis of the backscattering method for single-mode optical fibers," J. Opt. Soc. Am. **70**(8), 1010–1112 (1980).
2. M. Nakazawa, "Rayleigh backscattering theory for single-mode optical fibers," J. Opt. Soc. Am. **73**(9), 1175–1180 (1983).
3. K. I. Aoyama, K. Nakagawa, and T. Itoh, "Optical time domain reflectometry in a single-mode fiber," IEEE J. Quantum Electron. **17**(6), 862–868 (1981).
4. B. Yan, F. Dong, X. Zhang, X. Chen, J. Li, G. Tu, X. Chen, and B. Culshaw, "Application of pipeline safety real-time monitoring with distributed optical fiber sensing technique based on coherent Rayleigh backscattering," Chinese J. Quantum Electron. **30**(3), 341–347 (2013).
5. Y. Shang, Y. Yang, C. Wang, X. Liu, C. Wang, and G. Peng, "Optical fiber distributed acoustic sensing based on the self-interference of Rayleigh backscattering," Measurement **79**, 222–227 (2016).
6. S.-K. Liaw, S.-L. Tzeng, and Y.-J. Hung, "Rayleigh backscattering induced power penalty on bidirectional wavelength-reuse fiber systems," Opt. Commun. **188**(1-4), 63–67 (2001).
7. G. Talli, D. Cotter, and P. D. Townsend, "Rayleigh backscattering impairments in access networks with centralised light source," Electron. Lett. **42**(15), 877–878 (2006).
8. X. Zhu and S. Kumar, "Effects of Rayleigh backscattering in single-source bidirectional fiber-optic systems using different modulation formats for downstream and upstream transmission," Opt. Fiber Technol. **14**(3), 185–195 (2008).
9. B. Liu, X. Xin, L. Zhang, J. Yu, Q. Zhang, and C. Yu, "A WDM-OFDM-PON architecture with centralized lightwave and PolSK-modulated multicast overlay," Opt. Express **18**(3), 2137–2143 (2010).
10. R. G. H. van Uden, R. A. Correa, E. A. Lopez, F. M. Huijskens, C. Xia, G. Li, A. Schülzgen, H. de Waardt, A. M. J. Koonen, and C. M. Okonkwo, "Ultra-high-density spatial division multiplexing with a few-mode multicore fibre," Nat. Photonics **8**(11), 865–870 (2014).
11. P. Sillard, D. Molin, M. Bigot-Astruc, K. D. Jongh, and F. Achten, "Low-differential-mode-group-delay 9-LP-mode fiber," in *Optical Fiber Communication Conference* (Optical Society of America, 2015), paper M2C.2.
12. R. V. Jensen, L. Grüner-Nielsen, N. H. Wong, Y. Sun, Y. Jung, and D. J. Richardson, "Demonstration of a 9 LP-mode transmission fiber with low DMD and loss," in *Optical Fiber Communication Conference* (Optical Society of America, 2015), paper W2A.34.
13. T. Mori, T. Sakamoto, M. Wada, T. Yamamoto, and F. Yamamoto, "Low DMD four LP mode transmission fiber for wide-band WDM-MIMO system," in *Optical Fiber Communication Conference* (Optical Society of America, 2013), paper OTh3K.1.
14. V. A. Sleiffer, P. Leoni, Y. Jung, H. Chen, M. Kuschnerov, S. Alam, M. Petrovich, F. Poletti, N. V. Wheeler, N. Baddela, J. Hayes, E. Numkam Fokoua, D. J. Richardson, L. E. Gruner-Nielsen, Y. Sun, and H. de Waardt,

#262133 Received 29 Mar 2016; revised 19 May 2016; accepted 22 May 2016; published 26 May 2016

"Ultra-high capacity transmission with few-mode silica and hollow-core photonic bandgap fibers," in *Optical Fiber Communication Conference* (Optical Society of America, 2014), paper Tu2J.3.
15. N. K. Fontaine, R. Ryf, H. Chen, A. V. Benitez, B. Guan, R. Scott, B. Ercan, S. J. B. Yoo, L. E. Grüner-Nielsen, Y. Sun, R. Lingle, E. Antonio-Lopez, and R. Amezcua-Correa, "30×30 MIMO transmission over 15 spatial modes," in *Optical Fiber Communication Conference* (Optical Society of America, 2015), paper Th5C.1.
16. T. Kodama, T. Isoda, K. Morita, A. Maruta, R. Maruyama, N. Kuwaki, S. Matsuo, N. Wada, G. Cincotti, and K. Kitayama, "First demonstration of a scalable MDM/CDM optical access system," Opt. Express **22**(10), 12060–12069 (2014).
17. C. Xia, N. Chand, A. M. Velázquez-Benítez, Z. Yang, X. Liu, J. E. Antonio-Lopez, H. Wen, B. Zhu, N. Zhao, F. Effenberger, R. Amezcua-Correa, and G. Li, "Time-division-multiplexed few-mode passive optical network," Opt. Express **23**(2), 1151–1158 (2015).
18. T. Hu, J. Li, P. Zhu, Q. Mo, Y. Ke, C. Du, Z. Liu, Y. He, Z. Li, and Z. Chen, "Experimental demonstration of passive optical network based on mode-division-multiplexing," in *Optical Fiber Communication Conference* (Optical Society of America, 2015), paper Th2A.63.
19. B. Liu, L. Zhang, X. Xin, and J. Yu, "Symmetric Terabit WDM Pre-DFT OFDM access network using PCF-supercontinuum," Opt. Express **20**(22), 24356–24363 (2012).
20. B. Costa, P. Di Vita, P. Morra, U. Rossi, and B. Sordo, "Backscattering measurements in optical fibers: determination of mode distribution," Appl. Opt. **21**(23), 4186–4188 (1982).
21. R. Payne, "Modal distribution of backscattered light in a step-index multimode fibre," Electron. Lett. **17**(16), 568–570 (1981).
22. A. R. Mickelson and M. Eriksrud, "Theory of the backscattering process in multimode optical fibers," Appl. Opt. **21**(11), 1898–1909 (1982).
23. A. Li, A. A. Amin, X. Chen, and W. Shieh, "Reception of mode and polarization multiplexed 107-Gb/s CO-OFDM signal over a two-mode fiber," in *Optical Fiber Communication Conference* (Optical Society of America, 2011), paper PDPB8.
24. N. Hanzawa, K. Saitoh, T. Sakamoto, T. Matsui, S. Tomita, and M. Koshiba, "Demonstration of mode-division multiplexing transmission over 10 km two-mode fiber with mode coupler," in *Optical Fiber Communication Conference* (Optical Society of America, 2011), paper OWA4.
25. M. Nakazawa, M. Yoshida, and T. Hirooka, "Measurement of mode coupling distribution along a few-mode fiber using a synchronous multi-channel OTDR," Opt. Express **22**(25), 31299–31309 (2014).
26. Z. Wang, H. Wu, X. Hu, N. Zhao, Z. Yang, F. Tan, J. Zhao, Q. Mo, and G. Li, "Rayleigh backscattering in few-mode optical fibers," In *Optical Fiber Communication Conference* (Optical Society of America, 2016), paper W4F.6.
27. D. Yu, S. Fu, M. Tang, and D. Liu, "Mode-dependent characteristics of Rayleigh backscattering in weakly-coupled few-mode fiber," Opt. Commun. **346**, 15–20 (2015).
28. S. G. Leon-Saval, N. K. Fontaine, J. R. Salazar-Gil, B. Ercan, R. Ryf, and J. Bland-Hawthorn, "Mode-selective photonic lanterns for space-division multiplexing," Opt. Express **22**(1), 1036–1044 (2014).
29. A. M. Velazquez-Benitez, J. C. Alvarado, G. Lopez-Galmiche, J. E. Antonio-Lopez, J. Hernández-Cordero, J. Sanchez-Mondragon, P. Sillard, C. M. Okonkwo, and R. Amezcua-Correa, "Six mode selective fiber optic spatial multiplexer," Opt. Lett. **40**(8), 1663–1666 (2015).
30. V. A. J. M. Sleiffer, Y. Jung, V. Veljanovski, R. G. H. van Uden, M. Kuschnerov, H. Chen, B. Inan, L. G. Nielsen, Y. Sun, D. J. Richardson, S. U. Alam, F. Poletti, J. K. Sahu, A. Dhar, A. M. J. Koonen, B. Corbett, R. Winfield, A. D. Ellis, and H. de Waardt, "73.7 Tb/s (96 x 3 x 256-Gb/s) mode-division-multiplexed DP-16QAM transmission with inline MM-EDFA," Opt. Express **20**(26), B428–B438 (2012).

1. Introduction

As one of dominant linear characteristics of optical fibers, Rayleigh backscattering (RB) results from small scale inhomogeneities of the local electric susceptibility, which act as induced dipole oscillators [1, 2]. Many applications based on the RB arising in optical fibers have been widely explored, such as optical time domain reflectometry (OTDR) [3], optical fiber pipeline safety monitoring [4], distributed acoustic sensing [5]. However, when it comes to fiber optical bi-directional transmission, RB becomes one of the dominant impairment sources [6–9]. Recently, few-mode fiber (FMF) has been widely investigated to avoid the capacity crunch of single mode fiber (SMF) [10–13]. Mode division multiplexing (MDM) transmission using the FMF can effectively increase the capacity of SMF by N times through the utilization of parallel spatial modes as independent information channels [14, 15]. As a new application, FMF is proposed for passive optical networks (PON) due to its potential to maximize the loss budget and the number of optical network units (ONUs). Two-mode fiber (TMF) based PON has been experimentally demonstrated [16–19]. Therefore, RB arising in the TMF needs careful analysis, because it brings transmission impairment for upstream data transmission. The RB in the SMF has been comprehensively investigated in early years, both theoretically and experimentally [1, 20]. For multi-mode fibers (MMFs), the mode dependent power distribution of RB was experimentally found to be determined by the forward

#262133 Received 29 Mar 2016; revised 19 May 2016; accepted 22 May 2016; published 26 May 2016

propagation mode [21]. Then, theoretical investigation was performed with an assumption of mode continuum for strongly-coupled MMF [22]. In such MMF, the RB is found to equally propagate among all the guided modes. However, the currently used TMF differs from traditional MMF, because the structure parameters are specially designed in order to optimize the mode profile and differential mode group delay (DMGD) [23, 24]. As a result, the RB of TMF should have specific mode dependent characteristics. Although some work on the characterization of RB arising in the FMF have been reported recently [25, 26], the mode dependent characteristics of RB in the FMF are not comprehensively investigated. The backscattering power and corresponding mode dependent power distribution, as well as the relationship with specific forward propagation mode in various kinds of FMFs, still need to be explored. Moreover, the mode crosstalk induced by the mode division multiplexer should be taken into account. Generally, the backscattering power and the recapture factor are two commonly used parameters to evaluate the RB arising in SMF [2]. However, for the FMF case, such two parameters are not able to illuminate the mode dependent characteristics. Therefore, we define two new parameters, the RB power ratio and the relative mode dependent power (RMDP) to illustrate the RB power value and corresponding power distribution among the guided modes. The RB power ratio is defined as the ratio of the received RB power to the input power at a specific mode. Meanwhile, the RMDP is defined as the ratio of the RB power at individual higher order mode to the RB power at LP_{01} mode. Recently, we have theoretically investigated the mode dependent characteristics of RB in weakly-coupled FMF [27]. The RB power ratio and the RMDP are found to be sensitive to the mode profile of forward propagation light. However, such two parameters are challenging to quantitatively characterize through experiment, due to the limitation of precisely selective mode excitation. As the development of mode division multiplexers, all-fiber photonic lantern (PL) [28, 29] makes the measurement of RB arising in the FMF much easier, if we can get the power transfer matrix of PL and successfully suppress the Fresnel reflection from the facet.

In this paper, we propose an easy implementation to precisely characterize the mode dependent characteristics of RB light in various kinds of TMFs. With the help of all-fiber PL, we experimentally characterize the total RB power ratio and the RMDP, when the light propagates at individual modes. After obtaining the power transfer matrix of the PL, we are able to mitigate the mode crosstalk of the PL. Three type of TMFs are explored, including the TMFs with positive and negative DMGDs, as well as large effective TMF. The influence of forward propagation mode on the RB light is illustrated for three kinds of TMFs. Finally, we compare the experimental characterization with the theoretical calculations, based on our recently proposed theoretical model.

2. Experimental setup and operation principles

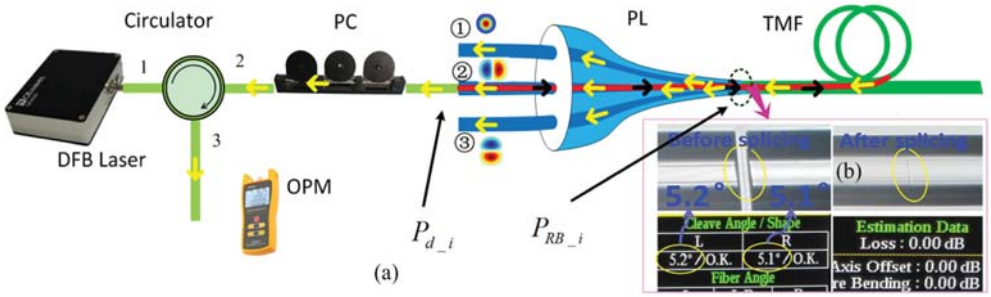

Fig. 1. Experimental setup. OPM: optical power meter; TMF: two-mode fiber; PC: polarization controller; PL: photonic lantern.

The experimental setup is shown in Fig. 1. The output of a distributed feedback (DFB) laser diode (LD) is launched into the PL via an optical fiber circulator. A polarization controller (PC) is used to optimize the state of polarization (SOP) of the fundamental mode, before we

#262133 Received 29 Mar 2016; revised 19 May 2016; accepted 22 May 2016; published 26 May 2016

complete mode selective conversion by the PL. The used PL is a 3-port device from Phoenix Photonics with a power transfer matrix T_{3PL}, as shown in Eq. (1), where R_{k_j} is the conversion efficiency of mode j (k = 1, 2, 3; j = 01, 11a, 11b), when we launch power at the input port k. The mode selectivity, which is defined as the power ratio of the power of expected mode to the power of all unexpected modes in dB form, is used to evaluate the performance of the PL. At the operation wavelength of 1550nm, the measured mode selectivity of PL is 16.80dB, 16.54dB, and 14.77dB for LP_{01}, LP_{11a}, and LP_{11b}, respectively. Then, the TMF under test is fusion spliced to the few-mode output end of the PL. The mode pattern can be monitored by an infrared charge coupled device (CCD) camera at the output end of the TMF. When we launch the continuous wave (CW) laser at the port 1 of the PL with an input power of P_{in}, the RB light can be collected from all three SMF input ports. Thus, we can separately detect the power by an optical power meter, which is defined as a vector of $\mathbf{P}_{d\_1}$, as shown in Eq. (2). The superscript $^{\mathrm{T}}$ represents the matrix transpose operation. The three elements $P_{d\_1\_k}$ (k = 1, 2, 3) are the corresponding power detected from individual SMF input port. Then we launch power at port 2 of the PL and follow the same procedure to obtain power vector $\mathbf{P}_{d\_2}$.

$$T_{3PL} = \begin{bmatrix} R_{1\_01} & R_{2\_01} & R_{3\_01} \\ R_{1\_11a} & R_{2\_11a} & R_{3\_11a} \\ R_{1\_11b} & R_{2\_11b} & R_{3\_11b} \end{bmatrix} \tag{1}$$

$$\mathbf{P}_{d\_i} = \begin{bmatrix} P_{d\_i\_1} & P_{d\_i\_2} & P_{d\_i\_3} \end{bmatrix}^{\mathrm{T}}, \quad (i = 1, 2) \tag{2}$$

Next we calculate the RB power ratio and the RMDP according to the detected power vectors and the power transfer matrix of the PL. Irrespective of the PL being mode selective or non-mode selective, the light propagates through the TMF under a combination of LP_{01} mode and LP_{11} mode. For the used PL, the power of forward LP_{01} mode and LP_{11} mode is determined by Eq. (3), when the DFB laser is connected to the input port i. Normally, both LP_{11a} and LP_{11b} mode superpose as one LP_{11} mode in the TMF. Therefore, it is only necessary to characterize LP_{11} mode, instead of discussing two spatially degenerate LP_{11} modes independently.

$$\begin{cases} P_{\mathrm{in}\_i\_01} = R_{i\_01} P_{in} \\ P_{\mathrm{in}\_i\_11} = R_{i\_11a} P_{in} + R_{i\_11b} P_{in} = R_{i\_11} P_{in} \end{cases} \quad (i = 1, 2) \tag{3}$$

The RB power at individual mode before propagating back to the PL can be obtained from Eq. (4), according to the power transfer matrix of the PL. $P_{RB\_i\_01}$, $P_{RB\_i\_11a}$, and $P_{RB\_i\_11b}$ are the powers of RB light at LP_{01}, LP_{11a}, and LP_{11b} mode, respectively. Thus the power of RB light at the LP_{11} mode is $P_{RB\_i\_11}$ ($P_{RB\_i\_11} = P_{RB\_i\_11a} + P_{RB\_i\_11b}$).

$$\mathbf{P}_{RB\_i} = \left(T_{3PL}^{\mathrm{T}}\right)^{-1} \cdot \mathbf{P}_{d\_i} = \begin{bmatrix} P_{RB\_i\_01} & P_{RB\_i\_11a} & P_{RB\_i\_11b} \end{bmatrix}^{\mathrm{T}}, (i = 1, 2) \tag{4}$$

Since RB is a linear property of FMF, the RB power, when the forward light propagates in arbitrary combination of the two modes, is simply the superposition of the RB power caused by both forward LP_{01} mode and forward LP_{11} mode. Therefore, it is meaningful to obtain the total RB power ratio and the RMDP, when only one designated mode is stimulated. When we launch power at one SMF input port, both LP_{01} mode and LP_{11} mode are excited with individual efficiency, because the mode selectivity of the PL is limited. In such case, the calculated RB power from Eq. (4) is the sum of the RB power caused by the forward propagation of both LP_{01} mode and LP_{11} mode. Here we introduce the parameter of RB power ratio, which is defined as the RB power at individual mode over the power of specific forward propagation mode. When the forward propagation light is LP_{01} mode alone, the RB mode ratios of backward LP_{01} mode and backward LP_{11} mode are t_{01_01} and t_{01_11}, respectively. Similarly, the RB mode ratios of backward LP_{01} mode and LP_{11} mode are t_{11_01} and t_{11_11}, respectively, when the forward light is at LP_{11} mode. According to the linear superposition

#262133 Received 29 Mar 2016; revised 19 May 2016; accepted 22 May 2016; published 26 May 2016

theory, Eq. (5) presents the relationship between the RB power ratio and the calculated RB power at individual mode. Obviously, we can derive t_{m_n} (m = 01, 11; n = 01, 11) according to Eq. (5). Finally, we can calculate the total RB power ratio and corresponding RMDP from the obtained t_{m_n}, as shown in Eqs. (6) and (7). Larger value of t_{m_n} equals to higher RB power, indicating more percent of the forward light is scattered and recaptured by the fiber and propagates back to the input end. Due to the low propogation loss of TMF, the two parameters becomes saturated when the TMF is longer than 25 km. Especially, the stable value of the RB power ratio has the same value as the recapture factor defined in [27]. Furthermore, such procedure can be further extended to the RB measurement of FMF with more higher order modes, as well as to the situation of optical pulse input to measure the RB at discrete point along the fiber.

$$\begin{bmatrix} R_{1\_01} & R_{1\_11} & 0 & 0 \\ R_{2\_01} & R_{2\_11} & 0 & 0 \\ 0 & 0 & R_{1\_01} & R_{1\_11} \\ 0 & 0 & R_{2\_01} & R_{2\_11} \end{bmatrix} \cdot \begin{bmatrix} t_{01\_01} \\ t_{11\_01} \\ t_{01\_11} \\ t_{11\_11} \end{bmatrix} \cdot P_{in} = \begin{bmatrix} P_{RB\_1\_01} \\ P_{RB\_2\_01} \\ P_{RB\_1\_11} \\ P_{RB\_2\_11} \end{bmatrix} \tag{5}$$

$$\text{total RB power ratio}_m = 10\log_{10}\left(\sum\nolimits_n t_{m\_n}\right), \quad (m = 01,11; n = 01,11) \tag{6}$$

$$\text{RMDP}_m = \frac{t_{m\_01}}{t_{m\_11}}, \quad (m = 01,11) \tag{7}$$

3. Experimental results and discussions

In this paper, we measure the RB arising in three kinds of TMFs with different mode properties, including the TMF with positive DMGD, the TMF with negative DMGD, and the TMF with large effective area. The detailed information of the TMFs under test is shown in Table 1. The first two are conventional TMFs which are utilized in current MDM transmission experiments [30], while the third one is specially designed TMF with large effective area to reduce impairment of nonlinearity.

Table 1. Parameters of TMFs Under Test.

	Length [km]	DMGD [ps/m]	Aeff_01 [μm^2]	Aeff_11 [μm^2]
TMF 1	29.98	0.039	96	96
TMF 2	29.98	-0.034	95	96
TMF 3	29.92	0.03	165	175
SMF	25.21	\	79	\

Initially, a short piece of TMF (2 m long) is fusion spliced to the output end of the PL. The output mode patterns captured by a CCD camera are shown in Figs. 2(a)-2(c) when we launch power from the three SMF input ports independently. The observed mode selectivity is about 16.75dB, 16.51dB, and 14.73dB for the three input ports, respectively. Then we spliced 29.98 km long TMF to the PL, the corresponding output mode patterns are shown in Figs. 2(d)-2(f). When we launch power at port 1, for the purpose of LP_{01} mode generation, the mode selectivity difference between the output of 2-m TMF and that of 29.98-km TMF is 4.5%, as shown in Figs. 2(a) and 2(d). When we launch power at port 2, for the purpose of LP_{11a} mode generation, no difference is observed except for the orientation rotation, as shown in Figs. 2(b) and 2(e). The mode selectivity difference is 4.86%. However, since two LP_{11} modes after long TMF transmission are no longer orthogonal, as shown in Figs. 2(e) and 2(f), we can conclude that the mode coupling between two LP_{11} modes with orthogonal orientations is very strong. In order to suppress the reflection from the splicing point and the Fresnel

#262133 Received 29 Mar 2016; revised 19 May 2016; accepted 22 May 2016; published 26 May 2016

reflection from the far-end facet of the TMF, we cleave the TMF with an angle of more than 5°, as shown in Fig. 1(b). Furthermore, since only single mode fiber (SMF) is used before the mode selective conversion by photonic lantern, we have done the fusion splicing of SMF to mitigate possbile Fresnel reflection.

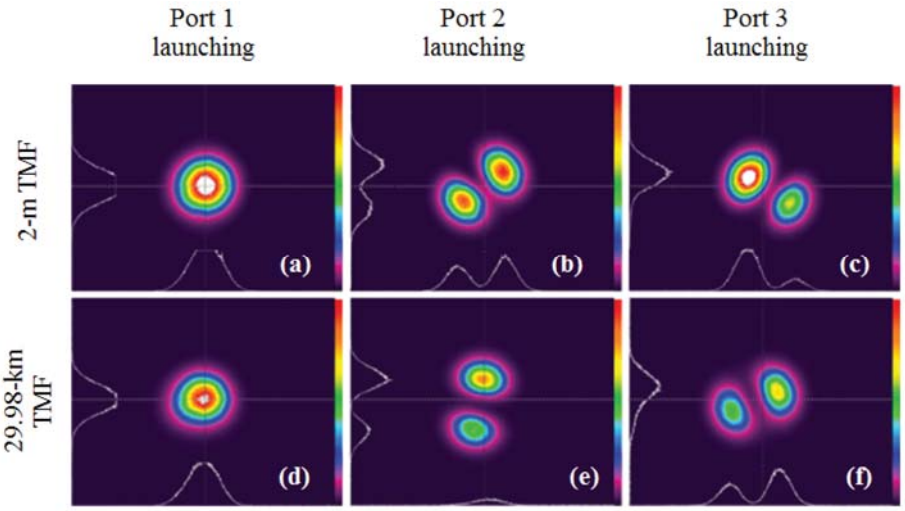

Fig. 2. Captured output mode patterns. (a)-(c) are for 2-m long TMF; (d)-(f) are for 29.98-km long TMF.

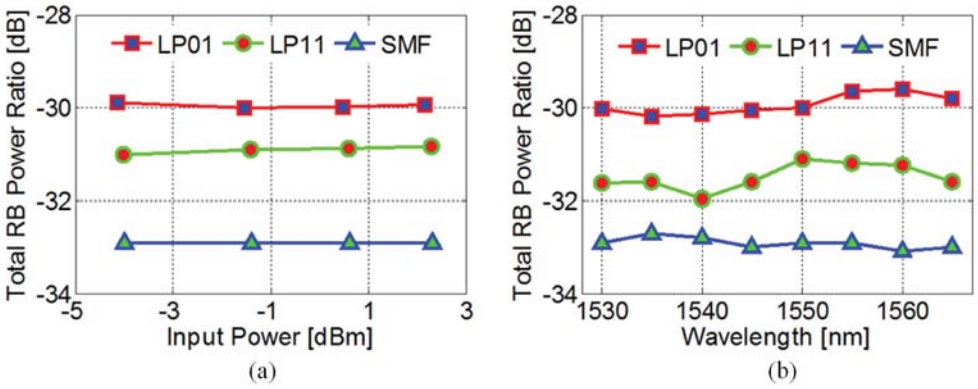

Fig. 3. Total RB power ratios in the TMF with positive DMGD. (a) with respect to the input power, (b) with repect to the operation wavelength.

For the characterization of TMF with positive DMGD, we first set the operation wavelength at 1550nm. When the forward light propagates at LP_{01} mode, the total RB power ratio of the TMF is measured to be −30dB, which is around 1 dB higher than the case of forward LP_{11} mode propagation. When we change the input power, the corresponding total RB power ratios are shown in Fig. 3(a). For the ease of comparision, we measure the total RB power ratio of the SMF as a reference. Obviously, the RB in the TMF is higher than that in the SMF by at least 2 dB. When the operation wavelength is swept over the C band, the total RB power ratios only have fluctuation of less than 0.89dB, as shown in Fig. 3(b). For the TMF, the total RB power is determined by the forward propagation mode. Moroever, the fundamental mode at forward propagation generates stronger RB power than that of the LP_{11} mode over the C band. The SMF has weaker RB power compared with the TMF with positive DMGD under test.

#262133 Received 29 Mar 2016; revised 19 May 2016; accepted 22 May 2016; published 26 May 2016

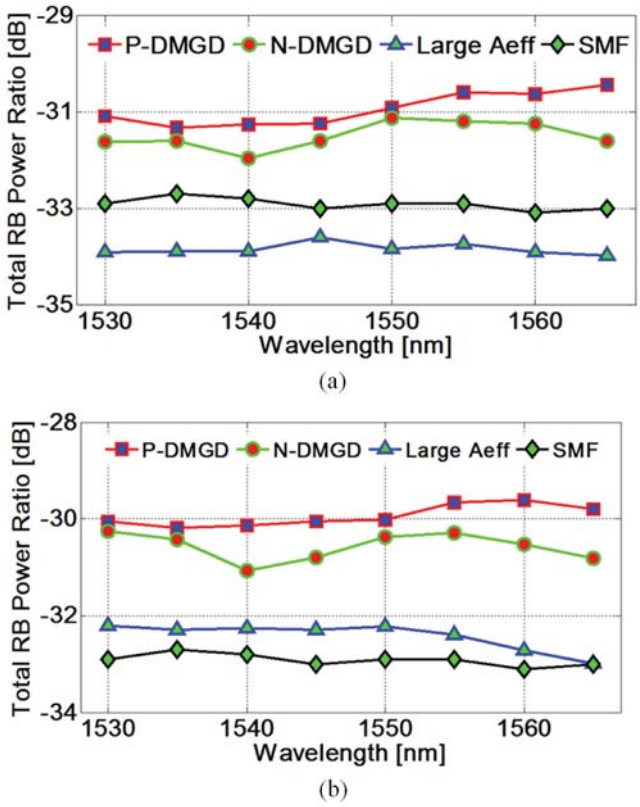

Fig. 4. Total RB power ratio of various TMFs. (a) under condition of LP_{01} mode forward propogation, (b) under condition of LP_{11} mode forward propagation.

Next we carry out characterization by another two types of TMFs. One is the TMF with negative DMGD and the other is the TMF with large effective area whose detailed information is described in Table 1. The total RB power ratio is shown in Figs. 4(a) and 4(b), when the forward light propagates at LP_{01} mode and LP_{11} mode, respectively. The results indicate that the three TMFs under test have different total RB power ratios. The TMF with positive DMGD and the TMF with negative DMGD have almost the same effective area of $96\mu m^2$ for both LP_{01} mode and LP_{11} mode. However, the total RB power of the TMF with positive DMGD is higher than that of the TMF with negative DMGD. Compared with the SMF, both have higher total RB power ratios irrespective of the forward propagation mode. The TMF with large effective area under test has lower RB power than that of the TMF with small effective area. When the forward light propagates at LP_{01} mode, the total RB power ratio is higher than that of the SMF by 0.4~0.7 dB. However, when the forward light is at LP_{11} mode, the total RB power ratio is lower than that of the SMF by around 1 dB. The total RB power is mainly determined by the power distribution of the forward propagation modes. Larger effective area means that the transverse field extends further away from the center of the fiber. Thus, the power density at the core becomes weak. According to the statistic model of the inhomogeneities, the mode with dense power distribution at the core has greater recapture factor of the backward Rayleigh scattering [2]. We believe this is the reason why the RB power of the TMF with larger effective area is lower than that of the TMF with smaller effective area. Meanwhile, both the TMF with positive DMGD and the TMF with negative DMGD have a graded refractive index profile with different α parameter. Although two kinds of TMFs have almost the same effective area, the TMF with positive DMGD has larger α parameter than that of the TMF with negative DMGD, indicating of higher density of the Germanium doping at the core area [13]. Consequently, the inhomogeneity at the core

#262133 Received 29 Mar 2016; revised 19 May 2016; accepted 22 May 2016; published 26 May 2016

region is more severe than that of the TMF with negative DMGD. Therefore, the TMF with positive DMGD has a little bit larger RB power, compared with the TMF with negative DMGD.

Next we focus on the mode dependent power distribution of RB light for the three types of TMFs under test, and the measured RMDP is shown in Fig. 5. The legend "P", "N", and "L" represents the fiber with positive DMGD, negative DMGD, and large effective area, respectively, while "-01" and "-11" mean the scenarios of forward light propagation at LP_{01} and LP_{11} mode, respectively. When RMDP is larger than 1.0, the backscattering light propagates mainly at the fundamental mode, while the RMDP of smaller than 1.0 indicates that the RB light exists mainly at LP_{11} mode. Moreover, the RB light is found to propagate at every guided mode of the TMF with different power proportions. In particular, the mode having the same mode profile with the forward propagation one has the largest power proportion. When the forward light propagates at the fundamental mode, more than 50% of the RB power exists in LP_{01} mode (RMDP>1.0). On the contrary, when the forward light is in LP_{11} mode, the percentage of RB power in LP_{01} mode is smaller than 33% (RMDP≤0.5). Interestingly, the TMF with positive DMGD and the TMF with negative DMGD almost have the same RMDP curve, although they have different total RB power. However, the TMF with large effective area has different results. The RMDP difference between two guided modes is larger than that of the TMFs with smaller effective area. Although the mode dependent power distribution is different due to various fiber refractive index profiles, the backscattering light always propagates mainly at the mode, which is the same with the forward one.

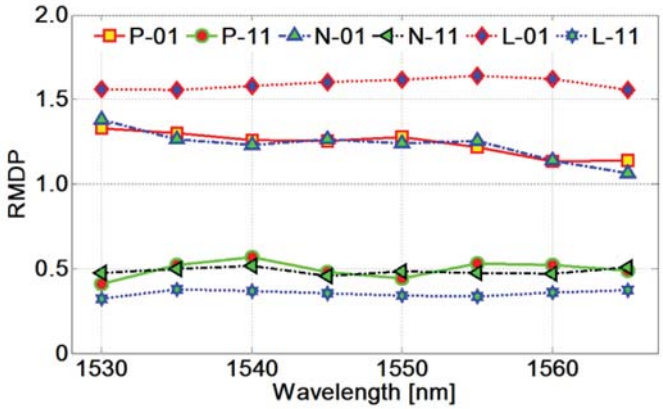

Fig. 5. RMDP of three TMFs under test.

Finally we compare the experimental results with the theoretical calculations [27]. When the operation wavelength is swept over the C band, the experimentally obtained total RB power agrees well with the theoretical ones for all the TMFs under test, as shown in Figs. 6(a)-6(f). Especially for the SMF, the experimental results and the theoretical ones are almost the same. Taking the TMF with positive DMGD as an example, the comparisons are shown in Fig. 6(a). The largest deviations between the experimental total RB power ratios and theoretical ones are 0.74dB, 0.63dB, and 0.34dB, under condition of LP_{01} mode forward propagation, LP_{11} mode forward propagation, and SMF propagation, respectively. As for the mode dependent power distribution, the RMDP deviation is a little larger. The theoretical RMDP overestimates the experimental ones, as shown in Fig. 6(b). When the light propagates forward at the fundamental mode, the deviation is about 15% over the C band. However, when the forward light propagates at LP_{11} mode, the deviation is around 18%. The deviation mainly comes from the state of polarization (SOP) imperfection of the input light. Since LP_{11} mode is a linearly polarized mode in the TMF, we need to adjust the SOP of input light to be linearly polarized when we measure the power transfer matrix of the PL. If the SOP of input light is not linearly polarized, the measured power transfer matrix has a fluctuation

#262133 Received 29 Mar 2016; revised 19 May 2016; accepted 22 May 2016; published 26 May 2016

accordingly. When we carry out the RB measurement, the SOP of input light may deviate from the perfect linear polarization. Therefore, the obtained total RB power ratio and corresponding RMDP by Eqs. (5)-(7) have a small deviation from the theoretical calculations.

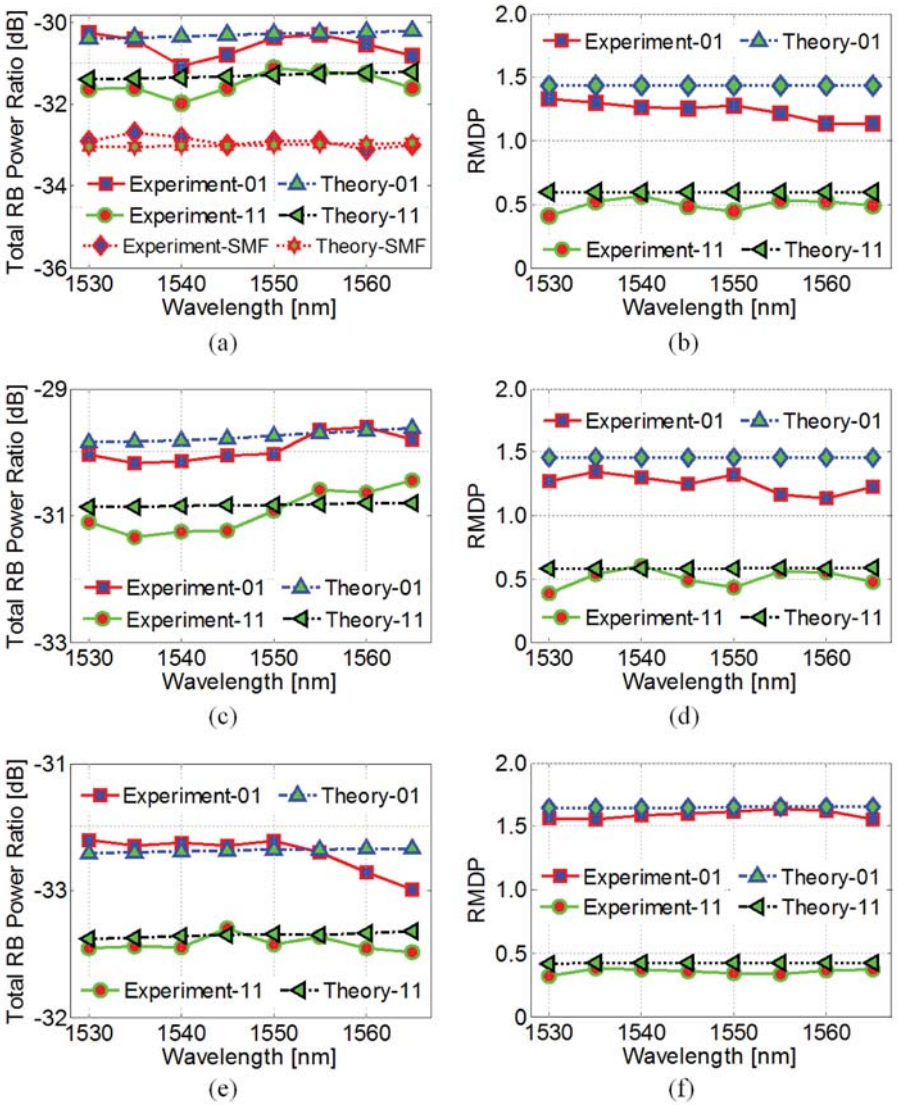

Fig. 6. Comparison of experimental characterization and theoretical calculations. (a), (c), and (e) are total RB power ratios for the TMF with positive DMGD, negative DMGD, large effective area, respectively; (b), (d), and (f) are RMDPs for the TMF with positive DMGD, negative DMGD, large effective area, respectively.

4. Conclusions

We have experimentally characterized the mode dependent characteristics of RB light arising in various TMFs with different structure parameters, with the help of all-fiber PL. By applying the power transfer matrix, we are able to deal with the mode crosstalk induced by the PL. The mode dependent power distribution of RB light is found to be determined by the forward propagation mode. The RB light in the TMF with small effective area is stronger than that of the SMF by at least 2dB. Moreover, the RB light is found to occur at all guided modes

#262133 Received 29 Mar 2016; revised 19 May 2016; accepted 22 May 2016; published 26 May 2016

in the TMF with individual power proportions. The RB light with the same mode profile of forward propagation mode has largest power than other guided modes. The experimental characterization agrees well with the theoretical calculations. The deviation of total RB power ratio is smaller than 0.74dB, while the maximum RMDP deviation is found to be around 18%.

Acknowledgments

This work was partially supported by the 863 High Technology Plan (2013AA013402), the National Natural Science Fundation of China (61275068, 61331010), the NOW Dutch photonics PhD program, and ZTE Industry-Academia-Research Cooperation Funds.

#262133 Received 29 Mar 2016; revised 19 May 2016; accepted 22 May 2016; published 26 May 2016